

## Article

# Study on Preparation and Properties of PNIPAm/PPy Hydrogel Hygroscopic Material for Solid Dehumidification System

Jinlin Liu, Yu Wang \* , Zilong Zhong, Zhou Zhou, Dongliang Chen, Weijie Wang and Shuaixing Mai

College of Urban Construction, Nanjing Tech University, Nanjing 211816, China; 19802657568@163.com (J.L.); zl\_zhong01@163.com (Z.Z.); 18851030801@163.com (Z.Z.); 15002881198@163.com (D.C.); hotliwell72@163.com (W.W.); 18851915590@163.com (S.M.)

\* Correspondence: yu-wang@njtech.edu.cn; Tel.: +86-025-83239533

**Abstract:** Air-conditioning systems account for 40–60% of the energy consumption of buildings, and most of this figure corresponds to the cooling and dehumidification process of air-conditioning units. Compared with traditional compressed air-conditioning systems, solid adsorption dehumidification systems possess good potential to improve indoor air quality and reduce buildings' energy consumption. However, there are still some problems that prevent the use of solid adsorption dehumidification systems, such as their complexity and high regeneration temperatures. The key to solving the above problem is the discovery of more suitable adsorbents. In this paper, poly N-isopropylacrylamide/polypyrrole (PNIPAm/PPy) hydrogel was selected as the research object, and the performance of the dehumidification material and its potential for application in solid dehumidification systems were studied. It was found that the pore structure of PNIPAm/PPy was relatively complex and that there were abundant pores with uneven pore sizes. The minimum pore size was about 4  $\mu\text{m}$ , while the maximum pore size was about 25  $\mu\text{m}$ , and the pore sizes were mostly distributed between 8 and 20  $\mu\text{m}$ . Abundant and dense pores ensure good hygroscopic and water-releasing properties of the resulting hydrogel. The PPy inside the hydrogel acts as both a hygroscopic and photothermal agent. In an environment with a relative humidity of 90%, 60%, and 50%, the hygroscopic efficiency of PNIPAm/PPy reached 80% in about 75, 100, and 120 min, and the corresponding unit equilibrium hygroscopic capacity values were 3.85 g/g, 3.72 g/g, and 3.71 g/g, respectively. In the initial stage, the moisture absorption increased with the increase in time; then, the increase in moisture absorption decreased. When the temperature was below 40 °C, the hygroscopic performance of PNIPAm/PPy was almost temperature-independent. The PNIPAm/PPy with different thicknesses showed similar moisture absorption efficiency. The lowest desorption temperature of PNIPAm/PPy was 40 °C, which indicates that low-grade energy can be used for material desorption. And the higher the temperature, the faster the desorption rate of PNIPAm/PPy and the higher the desorption amount. It can be seen that the PNIPAm/PPy hydrogel presents good desorption performance and can be used repeatedly.

**Keywords:** heat and mass transfer in porous media; dehumidification material; hydrogel; solid dehumidification system; hygroscopic efficiency; desorption performance



**Citation:** Liu, J.; Wang, Y.; Zhong, Z.; Zhou, Z.; Chen, D.; Wang, W.; Mai, S. Study on Preparation and Properties of PNIPAm/PPy Hydrogel Hygroscopic Material for Solid Dehumidification System. *Energies* **2023**, *16*, 5112. <https://doi.org/10.3390/en16135112>

Academic Editors: Guojun Yu, Huijin Xu and Mahmoud Bourouis

Received: 2 June 2023

Revised: 28 June 2023

Accepted: 30 June 2023

Published: 2 July 2023



**Copyright:** © 2023 by the authors. Licensee MDPI, Basel, Switzerland. This article is an open access article distributed under the terms and conditions of the Creative Commons Attribution (CC BY) license (<https://creativecommons.org/licenses/by/4.0/>).

## 1. Introduction

In developed countries, Heating Ventilation and Air Conditioning (HVAC) energy consumption accounts for 65% of buildings' energy consumption. As is known in this field, building energy consumption accounts for 35.6% of the total energy consumption among all sectors. Therefore, HVAC energy consumption accounts for up to 22.75% of the total level of energy consumption, and HVAC systems account for most of the energy consumed in the building operation stage [1]. In China, air-conditioning systems account for 40–60% of buildings' energy consumption [2], and this energy is mainly consumed by the air-cooling and dehumidification processes of air-conditioning units.

Among the commonly used air-conditioning and dehumidification technologies, condensation dehumidification systems tend to retain condensate water, mold, and other harmful substances. The system components of membrane dehumidification systems suffer from low permeability, poor strength, and high manufacturing costs [3]. The liquid desiccants commonly used in solution dehumidification have poor physical and chemical stability, and some are even corrosive or toxic [4]. Therefore, solid adsorption dehumidification has been vigorously developed in the field of HVAC. This system reduces indoor air humidity by directly absorbing water vapor in the air. The core component of solid desiccant dehumidification is a porous solid dehumidification material with a large specific surface area. The system uses the hydrophilic property of the dehumidification material to absorb the moisture in the air in order to reduce air humidity [5]. The dehumidification efficiency of a solid desiccant is high and low-grade heat source that can be used to regenerate materials, thus saving energy [6]. The most widely used solid desiccant dehumidification product is the wheel dehumidification system. The main components of the wheel dehumidification system are a dehumidification wheel, a rotating shaft, a motor, a dehumidification fan, a regenerative fan, and a heater [7]. Jin et al. [8] evaluated a solid desiccant dehumidifier equipped with an adsorbent-powder-coated heat exchanger (pchx) by testing the basic performance of the dehumidifier and the variation in the performance parameters under experimental conditions. The study found that the dehumidification system increased the floor area and cost and presented poor economic aspects. Compared with traditional compressed air-conditioning systems, solid adsorption dehumidification systems offer good potential for improving indoor air quality and reducing buildings' energy consumption, but they still face challenges such as their complexity and high regeneration temperatures [9]. The key to the successful application of this system is the discovery of a more suitable adsorbent.

The dehumidification material employed plays an important role in solid dehumidification air-conditioning systems. The dehumidification and purification performance of such systems is directly related to the characteristics of the dehumidification material. The energy consumption of a system also depends on the characteristics of the dehumidifying material. Commonly used solid dehumidification materials include silica gel, molecular sieves, activated carbon, activated alumina, composite materials, etc. The research and development statuses of solid dehumidification air-conditioning systems and adsorbents were investigated and summarized as follows.

Yaningsih et al. [10] designed a honeycomb structure solid adsorption dehumidification system using dehumidification materials; this dehumidification system can be regenerated at 55 °C. However, the heat exchanger and desorption module are very large and occupy a great deal of floor area. Kumar et al. [11] concluded that changing the hydration conditions of silica gel, e.g., changing the catalysts and solution pH and employing materials that can modify colloids, would alter its porosity and specific surface area. Chung et al. [12] modified silica gel, added boron into it, and irradiated it with neutron flux in order to enlarge its pores, improve its adsorption of water vapor, and reduce its analytical energy consumption. Kuma et al. [13] used water glass as a binder to prepare silica gel/molecular sieve composites. However, this method suffers from some problems, such as the poor dispersion of the molecular sieve and difficult preparation.

Djaeni et al. [14] proposed a new method to study the adsorption of zeolite molecular sieves. It consists of using the heat energy released via adsorption to improve the ambient air temperature, thus improving the overall energy efficiency and driving force of the drying process and effectively reducing the amount of energy consumed through dehumidification. Tokatev et al. [15] prepared a new material by using  $\text{CaCl}_2$  to modify an MCM-41 molecular sieve and studied the heat storage property of this modified new material. The results showed that reducing the number of nanopores in the MCM-41 improved its performance. Griesinger et al. [16] conducted experiments on the thermal conductivity of zeolite by controlling the pressure and temperature of its environment.

Bareschino et al. [17] numerically simulated a solid dehumidification air-conditioning system using a new composite material—MIL101@GO-6(MILGO)—as the dehumidification wheel. The analysis showed that the MLGO-based air treatment unit is superior to the traditional silicone-based air treatment unit in terms of energy saving, environmental protection, and economy. Canivet et al. [18] divided the adsorption process of water molecules on MOFs materials into three adsorption mechanisms: (1) adsorption on metal clusters; (2) multilayer and cluster adsorption in pore channels; and (3) capillary condensation in pores.

Yoshida et al. [19] and others synthesized a comb-type grafted Poly N-isopropylacrylamide (PNIPAm) hydrogel by changing the monomer structure of the starting material. The resulting hydrogel had a faster moisture absorption rate but also a relatively slow expansion rate and unstable performance. Wu X S et al. [20] and others synthesized a PNIPAm hydrogel with small pores and a faster moisture absorption rate by using the solubility differences of hydroxypropyl cellulose at different temperatures. Fei Zhao et al. [21] proposed a super-moisture-absorbent gel (SMAG) combining hygroscopic and hydrophilic polymers with a water-retaining and hydrophilic gel, resulting in a product that was greatly superior to other materials. This SMAG reimagines water capture in polymer networks rather than employing vapor adsorption based on active surfaces as employed in other materials.

The above literature review shows that the main research directions in this field are the improvement of traditional porous solid materials to obtain new composite porous materials and the discovery and development of new dehumidification materials in order to acquire materials with the necessary energy-saving, environmental protection, economic, and highly adsorbent properties for addressing the current energy problems. However, the existing dehumidification materials all suffer from low hygroscopic efficiency and high desorption temperature.

Poly N-isopropylacrylamide (PNIPAm) is a typical temperature-sensitive hydrogel with a rich pore structure. It possesses good hydrophilicity due to the occurrence of hydrogen bonding when the temperature is lower than its Lower Critical Solution Temperature (LCST). However, when the external temperature is higher than its LCST, a phase transition occurs, the hydrogen bonding is weakened, the hydrophobic interaction between the isopropyl group and the main chain becomes dominant, and the water in the polymer is released [22].

Polypyrrole (PPy) has good environmental stability and hygroscopicity [23]. Since the PNIPAm hydrogel has poor hygroscopicity, we used in situ polymerization to polymerize the PNIPAm hydrogel to form an interpenetrating network. PPy captures water molecules in the air and then transfers the condensed water to the PNIPAm network for storage. Therefore, the combination of the above two materials can effectively improve the hygroscopicity and regeneration performance of the composite. PPy's moisture absorption capacity is much higher than that of commonly used moisture-absorbing materials such as silica gel and zeolite in solid dehumidification systems. Therefore, it has great energy-saving potential in the field of building dehumidification.

In this paper, a poly N-isopropylacrylamide/polypyrrole (PNIPAm/PPy) hydrogel was selected as the research object with which to conduct experimental research on the performance of dehumidification materials and the key parameters such as the regeneration temperature and the regeneration time of solid dehumidification systems.

## 2. Preparation of Hygroscopic Materials

### 2.1. Raw Materials and Experimental Instruments

The raw materials and reagents required for the experiment are listed in Table 1. In this experiment, N-isopropylacrylamide (NIPAm) was recrystallized with a benzene-n-hexane (1:1 v/v) mixed solvent. N',N'-methylene diacrylamide (BIS) was recrystallized with ethanol. Ammonium persulfate was recrystallized with deionized water. The other reagents used were not treated twice.

**Table 1.** Main raw materials and reagents.

Raw Material	Grade	Manufacturer
N-isopropylacrylamide (NIPAm)	Analytical purity	Maclean Biochemical Technology Co., Ltd., Shanghai, China
Acrylamide (AM)	Analytical purity	Maclean Biochemical Technology Co., Ltd., Shanghai, China
CaCO <sub>3</sub>	Analytical purity	Aladdin Reagent (Shanghai) Co., Ltd., Shanghai, China
N',N'-methylene diacrylamide (BIS)	Analytical purity	Aladdin Reagent (Shanghai) Co., Ltd., Shanghai, China
Ammonium persulfate (APS)	Analytical purity	Aladdin Reagent (Shanghai) Co., Ltd., Shanghai, China
Tetramethylethylenediamine	Analytical purity	Aladdin Reagent (Shanghai) Co., Ltd., Shanghai, China
Pyrrole (Py)	Analytical purity	Aladdin Reagent (Shanghai) Co., Ltd., Shanghai, China
Hydrochloric acid	Analytical purity	Shanghai Lingfeng Chemical Reagent Co., Ltd., Shanghai, China

## 2.2. Preparation Method of PNIPAm/PPy Hydrogel

A total of 567 mg of N-isopropylacrylamide (NIPAm) was mixed with 10 mL of deionized (DI) water and purged with nitrogen for 10 min; the resulting mixture was denoted as solution A. The bubbles in solution A were removed via centrifugation at 7000 RPM for 5 min.

Then, 1 mL of N',N'-methylene diacrylamide solution (30 mg/mL) and 500  $\mu$ L of ammonium persulfate solution (APS, 228 mg/mL) were added to solution A. Finally, 10  $\mu$ L of N,N-tetramethylethylenediamine was added as an accelerator, and sealed reaction polymerization was carried out for 12 h. The obtained PNIPAm hydrogel was immersed in hot deionized water (at a temperature of about 80 °C) for 12 h to remove the unreacted monomers. The purified PNIPAm hydrogel (with a volume of about 1 cm<sup>3</sup>) was immersed in hot deionized water (at a temperature of 80 °C) for complete contraction and then transferred to pyrrole solution overnight (pyrrole-to-water volume ratio 1:10).

The swollen hydrogel was washed in deionized water. The N-isopropylacrylamide/pyrrole (PNIPAm/Py) hydrogel was then immersed in a mixture of ammonium persulfate (228 mg), 37% hydrochloric acid (85  $\mu$ L), and 10 mL of deionized water. A mixed gel was formed via the in situ polymerization of NIPAm hydrogel overnight. Finally, the obtained PNIPAm/PPy was immersed in hot deionized water (about 80 °C) for 3 h to remove the unreacted monomers. The purification procedure was repeated 3 times. Figure 1a white hydrogel depicts the PNIPAm prepared, and Figure 2b black hydrogel depicts the PNIPAm/PPy prepared via the in situ polymerization of PPy in PNIPAm.

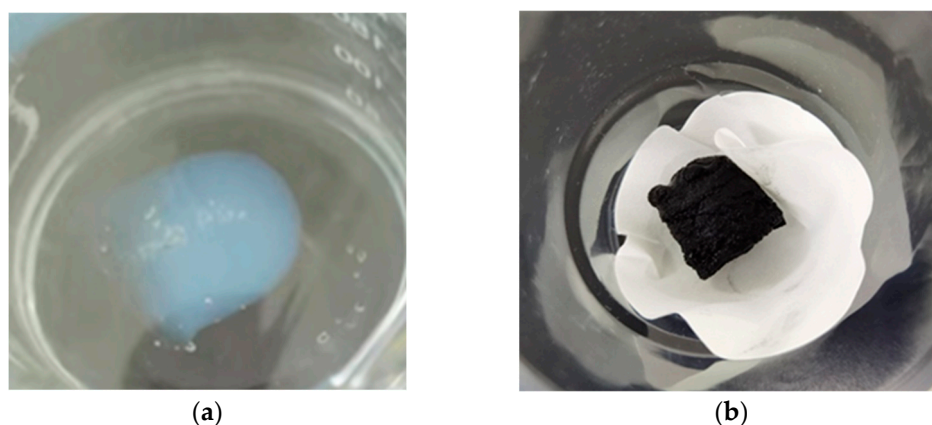


**Figure 1.** The prepared hydrogels. (a) The prepared PNIPAm hydrogel. (b) The prepared PNIPAm/PPy hydrogel.

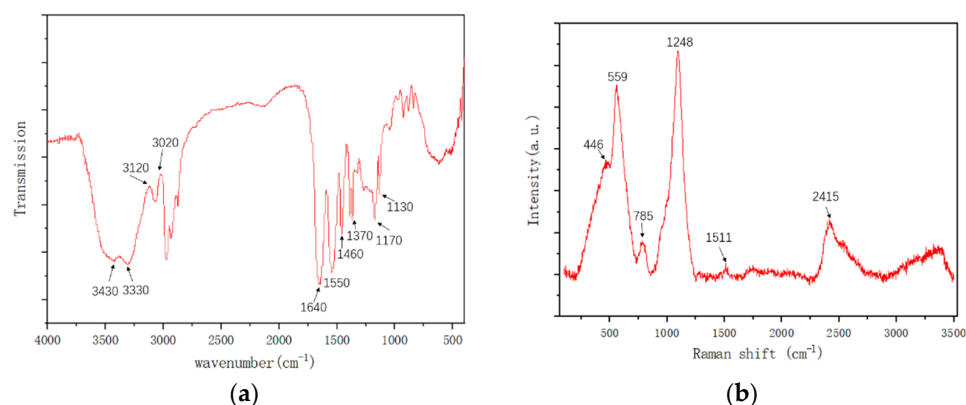


**Figure 2.** Infrared and Raman spectra of PNIPAm/PPy. (a) Infrared spectrum of PNIPAm/PPy. (b) Raman spectrum of PNIPAm/PPy.

Figure 2 shows the infrared and Raman spectra of PNIPAm/PPy. A strong absorption peak appears at  $3430\text{ cm}^{-1}$ , which corresponds to the stretching vibration peak of the  $\text{-NH}$  functional group in the PNIPAm hydrogel. The strongest absorption peak appears at  $1640\text{ cm}^{-1}$ , which corresponds to  $\text{C=O}$  in the PNIPAm gel, and an absorption peak with a lower intensity appears at  $1170\text{ cm}^{-1}$ , which is caused by the stretching vibration of the  $\text{C-C}$  skeleton in the isopropyl group in the PNIPAm gel. Accordingly, it can be inferred that there are hydrophilic amide groups  $\text{-CONH-}$  and hydrophobic isopropyl groups  $\text{-CH(CH}_3)_2\text{-}$  in the PNIPAm gel molecule. At the same time, there is a weak absorption peak at  $3120\text{ cm}^{-1}$ , indicating the presence of  $\text{=C-H}$  in the product, which, in turn, indicates that the monomer reaction yields PNIPAm. The wide peak at  $3330\text{ cm}^{-1}$  in Figure 2 is caused by the  $\text{N-H}$  stretching vibration of the pyrrole ring, and it partially overlaps the stretching vibration peak of the  $\text{N-H}$  functional group in the PNIPAm hydrogel. The characteristic peak at  $1550\text{ cm}^{-1}$  is attributed to the stretching of the  $\text{C=C}$  double bond. The weak peaks at  $1460\text{ cm}^{-1}$  and  $1170\text{ cm}^{-1}$  represent the plane deformations of  $\text{C-N}$  and  $\text{C-H}$  bonds, respectively. In addition, the peak generated at  $1130\text{ cm}^{-1}$  can be attributed to the stretching of the  $\text{C-C}$  bond.

### 3. Experimental Section

#### 3.1. Experimental Bench

A schematic diagram of the experimental bench is shown in Figure 3. The main experimental instruments are shown in Table 2. In the diagram, the enclosed test box simulates the closed space of a building, and the hygroscopic material is placed in the test tube. A humidifier with adjustable humidity is used to humidify the air, and the fan sends the wet air into the test tube. A temperature and humidity sensor is used to measure and control the set temperature and humidity.

**Table 2.** Main experimental instruments.

Instrument Name	Model	Manufacturer
Electronic hygograph	GL613	Yongkang Zhenmei Home Furnishings Co., Ltd., Jinhua, China
Electronic balance	SQP	Sartorius Scientific Instruments Co., Ltd., Göttingen, Germany
Vacuum-drying oven	DZF6020	Shanghai Boxun Industrial Co., Ltd., Shanghai, China
Reverse osmosis deionization pure water machine	Master-Q	Shanghai Hetai Instrument Co., Ltd., Shanghai, China
Humidifier	KZ-H861	Shenzhen Kangjiajia Intelligent Electric Appliance Technology Co., Ltd., Shenzhen, China
Axial fan	YY12038HBL2	Shenzhen Yongyihao Electronics Co., Ltd., Shenzhen, China
Vacuum freeze-dryer	LGJ-10	Shanghai Jipu Electronic Technology Co., Ltd., Shanghai, China
Scanning electron microscope	JSM-6510	Jieou Road (Beijing) Science and Trade Co., Ltd., Beijing, China

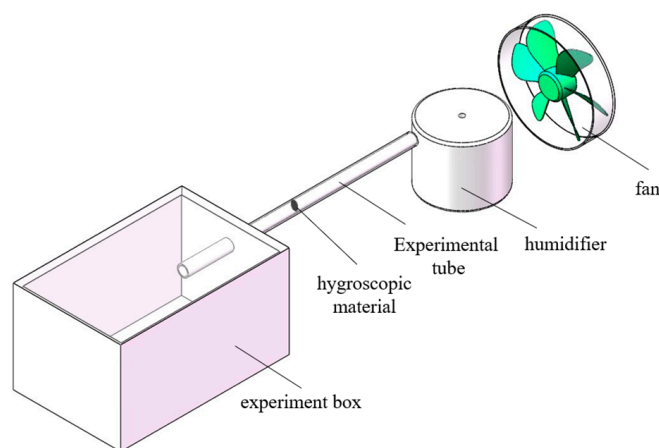


**Figure 3.** Experimental bench.

### 3.2. Material Characterization Test

The hygroscopic properties of hygroscopic materials are often evaluated and analyzed using indexes such as hygroscopic capacity and hygroscopic rate. Different temperatures, different relative humidities, and different thicknesses of materials all have a certain influence on hygroscopic performance. In this paper, by controlling the relative humidity, temperature, and material thickness and measuring the moisture absorption rate of PNIPAm/PPy hydrogel, its moisture absorption performance was analyzed (and is presented as follows).

**The influence of relative humidity on moisture absorption performance.** A PNIPAm/PPy hydrogel with a thickness of 2 mm was placed in a test tube; the temperature in the control chamber was 26 °C. The relative humidity in the control tube was 50%, 60%, and 90%. Air at different relative humidities was fed into the test tube through a fan. The weight change of the PNIPAm/PPy hydrogel was recorded every 5 min.

**The influence of temperature on moisture absorption performance.** A PNIPAm/PPy hydrogel with a thickness of 2 mm was placed in a test tube. The relative humidity in the control tube was 45%, and the temperature in the control chamber was 25 °C, 30 °C, and 35 °C. Air at different temperatures was fed into the test tube through a fan. The weight change of the PNIPAm/PPy hydrogel was recorded every 5 min.

**The Influence of size on hygroscopic performance.** Three kinds of PNIPAm/pPy hydrogels with thicknesses of 1 mm, 1.5 mm, and 2 mm were placed in the test tube to maintain the temperature of the tube at 26 °C and the relative humidity at 90%. Air with a relative humidity of 90% was fed into the test tube using a fan. The weight change of PNIPAm/PPy hydrogel was recorded every 5 min.

### 3.3. Material Regeneration Performance Test

After repeated uses, the water absorption capacity of a dehumidification material will gradually decrease. Desorption temperature, desorption amount, and the degree of water absorption after regeneration were used as indicators to investigate the regeneration performance of PNIPAm/PPy hydrogel. The procedures used to test the regeneration performance of the PNIPAm/PPy hydrogel are as follows:

**The lowest desorption temperature:** A 2 mm hydrogel was placed in an oven after hygroscopic saturation at relative humidities of 50%, 60%, and 90%. The change in the weight of the PNIPAm/PPy hydrogel was recorded every 2 min at 5 °C intervals. The temperature when the weight changed was regarded as the lowest desorption temperature of the material.

**Desorption quantity at different temperatures:** A 2 mm hygroscopic saturated PNIPAm/PPy hydrogel was placed into the oven to test the amount of PNIPAm/PPy hydrogel desorbed at 45 °C, 50 °C, 60 °C, 70 °C, and 80 °C at five constant temperatures. The change in weight of the PNIPAm/PPy hydrogel was recorded every 2 min after heating.

**Water absorption test after regeneration:** After hygroscopic saturation under a relative humidity of 90%, 1 mm, 1.5 mm, and 2 mm PNIPAm/PPy hydrogels were placed into an oven and heated at 80 °C for 1 h. Then, the physically adsorbed water on the surface was removed, and dry PNIPAm/PPy hydrogel was obtained. The moisture absorption performance of the hygroscopic material after regeneration was tested repeatedly.

The unit equilibrium hygroscopic capacity of the PNIPAm/PPy hydrogel hygroscopic material can be calculated using Formula (1) [24]:

$$q_e = \frac{m_1 - m}{m} \quad (1)$$

where  $q_e$  is the unit equilibrium moisture absorption of the PNIPAm/PPy hydrogel, which is given in g/g;  $m_1$  is the hygroscopic mass of the PNIPAm/PPy hydrogel in a certain state, which is given in g; and  $m$  is the mass of the PNIPAm/PPy hydrogel before the hygroscopic process, which is given in g.

The moisture absorption efficiency of the PNIPAm/PPy hydrogel hygroscopic material can be expressed by  $Q_s$  at a certain degree of relative humidity, as shown in Equation (2) [21]:

$$Q_s = \frac{m_1 - m}{m_s - m} \times 100\% \quad (2)$$

where  $Q_s$  is the moisture absorption efficiency of PNIPAm/PPy hydrogel, which is given in %;  $m_1$  is the hygroscopic mass of PNIPAm/PPy hydrogel in a certain state, which is expressed in g;  $m$  is the mass of PNIPAm/PPy hydrogel before the hygroscopic procedure; and  $m_s$  is the mass of PNIPAm/PPy hydrogel after hygroscopic saturation, g.

## 4. Results and Analysis

### 4.1. Structural Analysis of Hygroscopic Materials

The material was freeze-dried at a temperature of 223.15 K and an environmental pressure of 20 Pa so that the water in the material was completely removed while its microstructure was completely removed. Small samples were cut from the dried materials, their surfaces were sprayed with gold, and then they were observed under 10 kV voltage using a JSM-6510 scanning electron microscope.

Figure 4 shows the SEM surface topography and pore size distribution histogram inside the PNIPAm/PPy hydrogel, among which Figure 4a,b are the internal cross-section images of the hydrogel at 100 and 500 times magnification, respectively, and Figure 4c is the internal pore size distribution histogram of the hydrogel. From Figure 4a–c, it can be seen that there are abundant pores with uneven pore sizes inside the hydrogel. The minimum pore size is about 4 μm, the maximum pore size is about 25 μm, and the pore size is mostly distributed between 8–20 μm. The rich and dense pores increase the specific surface area of the material and ensure good hygroscopic and water-releasing properties of the hydrogel.

Figure 4d–f are scanning electron microscope images at magnifications of 1000 times, 5000 times, and 5000 times (in different positions), respectively. In the high-magnification microscopic images, there are relatively dense protrusions on the pore wall of the hydrogel; this is the PPy inside the hydrogel, which plays the role of a moisture absorption agent and a photothermal agent.

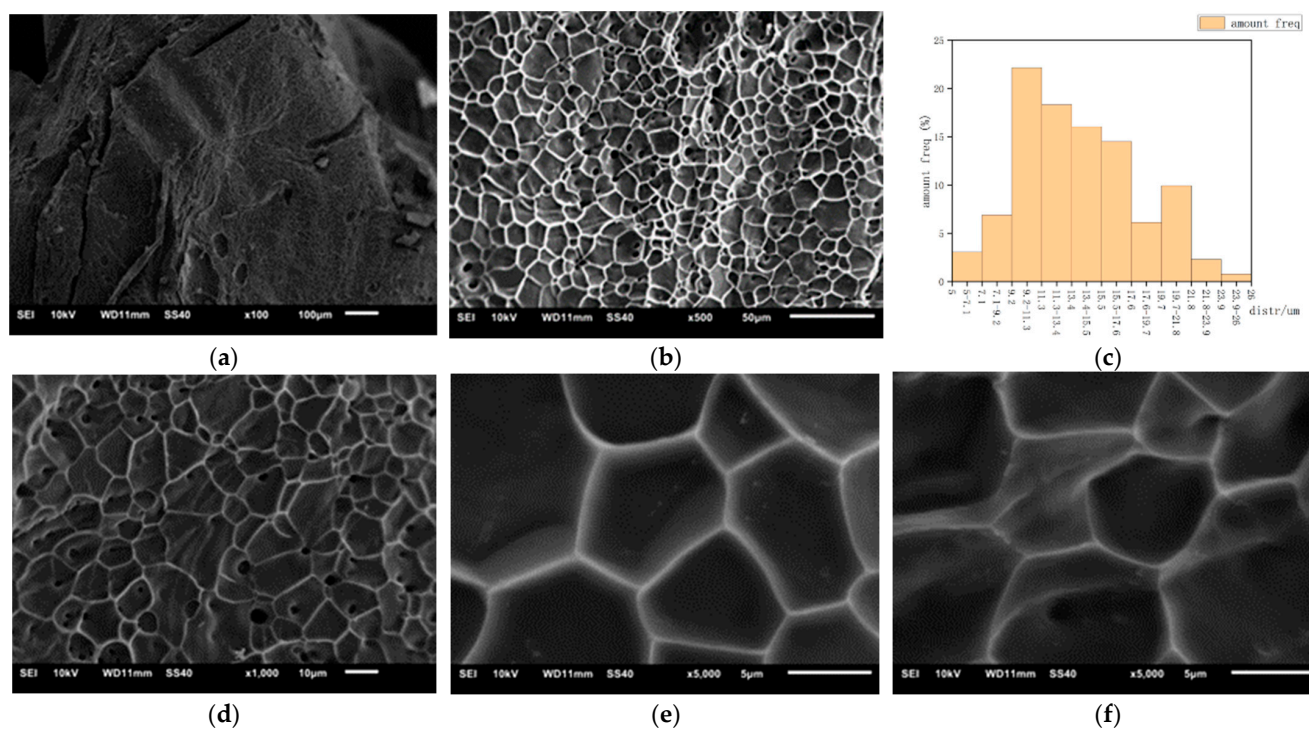


**Figure 4.** SEM images and histogram of pore size distribution of hydrogel at different magnifications. (a) PNIPAm/PPy magnified 100 times. (b) PNIPAm/PPy magnified 500 times. (c) Pore size distribution histogram of PNIPAm/PPy. (d) PNIPAm/PPy magnified 1000 times. (e) PNIPAm/PPy magnified 5000 times. (f) PNIPAm/PPy magnified 5000 times.

#### 4.2. Adsorption Property Analysis

##### 4.2.1. Effect of Relative Humidity (RH) on Hygroscopic Performance

Different relative humidities have a certain influence on hygroscopic performance. However, this influence is non-linearly dependent on the moisture-capturing rate and time. The moisture-capturing efficiency of PNIPAm/PPy can be represented by the ratio of moisture content and the corresponding saturated moisture content ( $Q_s$ ) at a certain relative humidity (RH).

As shown in Figure 4, the hydrogel absorbs moisture from the air with relative humidities (RHs) of 90%, 60%, and 50%. It takes 75, 100, and 120 min for the adsorption saturation rate of the PNIPAm/PPy hydrogel to reach 80% at each RH value, respectively, and the corresponding hygroscopic amounts are 3.85 g/g, 3.72 g/g, and 3.71 g/g, respectively.

It can be seen from Figure 4 that in the initial stage, the moisture absorption rate increases with the increase in time; then, the increase rate of moisture absorption decreases. The higher the relative humidity (RH), the faster the hygroscopic speed, which can be explained according to the probability of collision. In the initial hygroscopic stage, all adsorption sites in the pores of the hygroscopic material PNIPAm/PPy are empty, and the probability of water molecules hitting adsorption vacancies is relatively high. As the adsorption process progresses, the adsorption vacancies gradually become occupied and increasingly fewer in number. The probability of water molecules hitting vacancies decreases, and the increase in moisture absorption gradually decreases until reaching saturation. During the moisture absorption process, the volume of PNIPAm/PPy increases with the increase in moisture absorption, but the density of PNIPAm/PPy remains almost at 1 g/cm<sup>3</sup>. Generally, in solid dehumidification systems, devices equipped with hygroscopic materials have a certain pore space. As a result, an increase in volume has no impact on the system.

Three sets of data were tested, and the average values were considered to be the final values. As shown in Table 3 and Figure 5, the maximum error between the three sets of data and the average value is approximately within  $\pm 0.0002$  g, and the error of the electronic balance is  $\pm 0.0002$  g. Upon comparing the two errors, we consider the error of the electronic balance to be greater than or equal to the measurement error. The error line is almost invisible in Figure 5a, which has no impact on the trend of the curve; even if a portion of the data captured in Figure 5b is magnified, the error line is not obvious. Therefore, we will no longer emphasize the error line in the following text.

**Table 3.** Changes in PNIPAm weight over time under different humidities in three sets of experiments.

Time (min)	Number of Groups	RH (%)		
		50	60	90
75	1	1.0006	1.0523	1.1597
	2	1.0008	1.0521	1.1599
	3	1.0007	1.0524	1.1601
	average value	1.0007	1.0523	1.1599
100	1	1.0761	1.1313	1.2325
	2	1.0758	1.1312	1.2326
	3	1.0758	1.1313	1.2324
	average value	1.0759	1.1313	1.2325
120	1	1.1236	1.1814	1.2904
	2	1.1232	1.1813	1.2902
	3	1.1234	1.1811	1.2901
	average value	1.1234	1.1813	1.2902

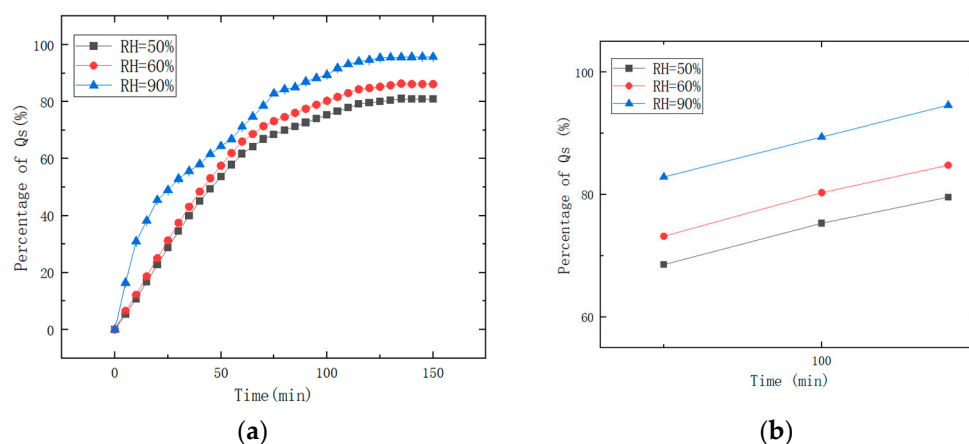


**Figure 5.** Moisture content variation represented by the percentage of the corresponding saturated water content ( $Q_s$ ) of each sample over time. (a) Moisture absorption performance changes of PNIPAm/PPy with different RH values within 0–150 min. (b) Moisture absorption performance changes of PNIPAm/PPy with different RH values at 70, 75, and 80 min.

#### 4.2.2. Effect of Temperature on Hygroscopicity

Traditional porous hygroscopic materials are sensitive to temperature adsorption because the diffusion of water vapor from the air into a nanopore is the rate-determining step. To verify the different moisture-capturing mechanisms of PNIPAm/PPy under different temperatures, the experimental temperatures were set as 25 °C, 30 °C, and 35 °C, with the other conditions remaining the same. As shown in Figure 6, the experimental curves almost coincide at the temperatures of 25 °C, 30 °C, and 35 °C. The results show that the hygroscopicity of PNIPAm/PPy was almost independent of temperature when the temperature was below 40 °C, which means that in terms of the application conditions of building air-conditioning systems, PNIPAm/PPy shows steady hygroscopicity.

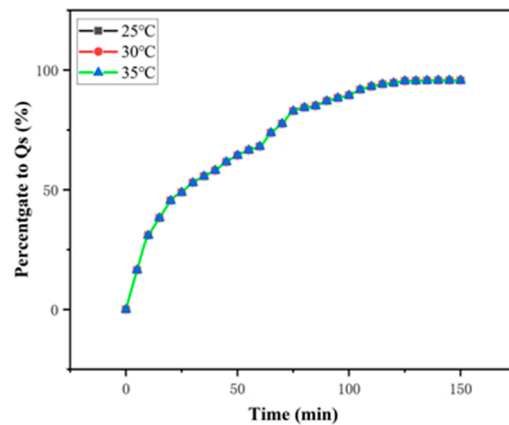


**Figure 6.** The moisture-capturing behavior of PNIPAm/PPy at different temperatures.

#### 4.2.3. Effect of Size on Hygroscopicity

As shown in Figure 7a,b, under the same operating conditions, the 1 mm, 1.5 mm, and 2 mm PNIPAm/PPy samples were subjected to moisture absorption. As shown in Figure 6, at 90 min, the moisture absorption efficiencies were 89.01%, 87.31%, and 87.07%, respectively. The experimental results showed that thickness had a certain effect on the moisture absorption performance of PNIPAm/PPy. The lower the thickness, the higher the moisture absorption efficiency. However, the variations show overall similarity.

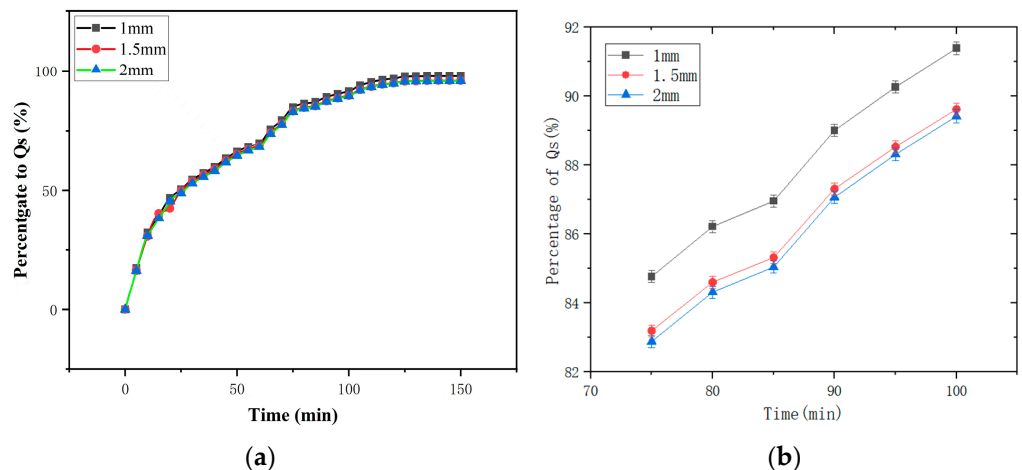


**Figure 7.** The moisture-capturing behavior of PNIPAm/PPy with different thicknesses. (a) Moisture absorption performance changes of PNIPAm/PPy with different thicknesses within 0–150 min. (b) Moisture absorption performance changes of PNIPAm/PPy with different thicknesses within 75–100 min.

#### 4.3. Regeneration Performance Analysis

Heating is a common regeneration method. The PNIPAm/PPy hygroscopic material increases the kinetic energy of water molecules by increasing the temperature in order to remove water molecules from the PNIPAm/PPy desorption site. The desorption temperature of traditional porous solid materials may exceed 100 °C, leading to energy wastage. If the desorption temperature of the PNIPAm/PPy hygroscopic material is greatly decreased, significant energy savings may be yielded.

##### 4.3.1. Lowest Desorption Temperature

As shown in Figure 8, the weight of PNIPAm/PPy was almost unchanged before reaching a temperature of 40 °C. At a temperature of 40 °C, the weight of PNIPAm/PPy began to change. The results show that the lowest desorption temperature of PNIPAm/PPy

was 40 °C and that the higher the temperature, the faster the desorption speed of PNIPAm/PPy. The lower desorption temperature observed indicates that low-grade energy can be used for desorption.

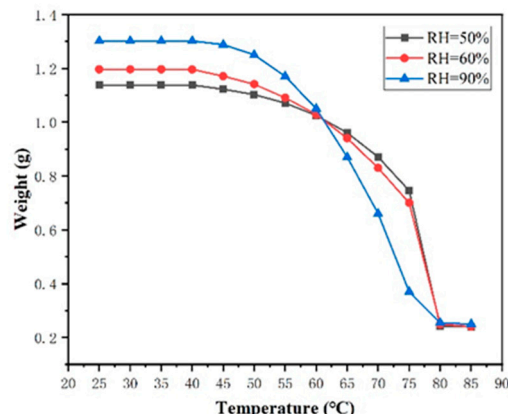


Figure 8. Change in weight of PNIPAm/PPy with temperature after moisture absorption saturation.

The main driving forces of phase transitions are hydrogen bonding and hydrophobic interactions, which change due to the influence of external conditions on the hydrophilic/hydrophobic equilibrium of the network. PNIPAm is a typical thermosensitive hydrogel. When the external temperature is lower than its LCST, it shows good hydrophilicity due to the influence of hydrogen bonding and Van der Waals forces. When the external temperature is higher than its LCST, a phase transition occurs, the hydrogen bond effect is weakened, the hydrophobic effect between the isopropyl group and the main chain becomes dominant, and the water in the polymer is released. Due to factors such as phase change heat absorption, the actual lowest desorption temperature of PNIPAm/PPy is around 40 °C.

#### 4.3.2. Effect of Temperature on Desorption

As mentioned in the main text, different relative humidities have a certain influence on the amount of water desorbed. As shown in Figure 9, the complete desorption times of the PNIPAm/PPy hydrogel at 45 °C, 50 °C, 60 °C, 70 °C, and 80 °C were 300 min, 220 min, 150 min, 100 min, and 60 min, respectively. The results show that the higher the temperature, the higher the desorption amount and the faster the desorption rate.

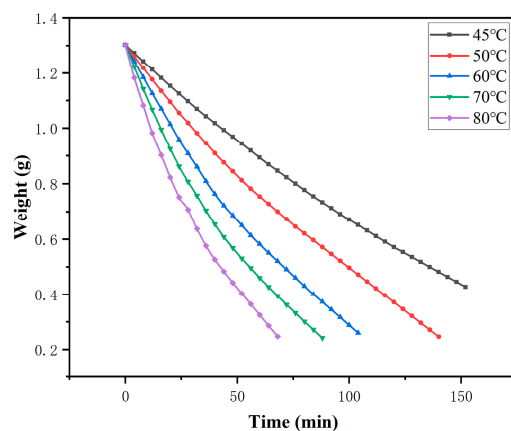
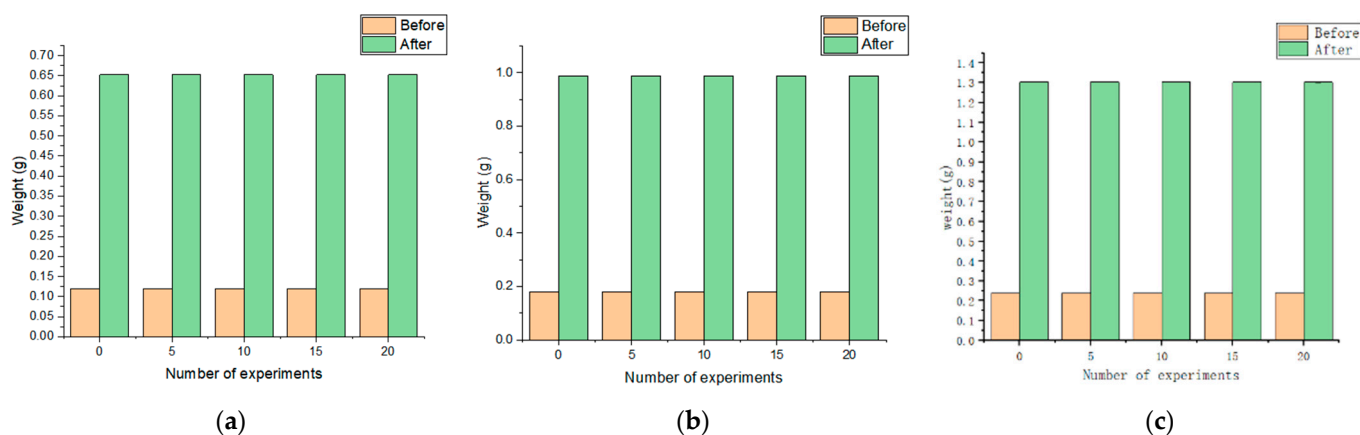


Figure 9. Changes in weight of PNIPAm/PPy over time at different desorption temperatures.

### 4.3.3. Effect of Desorption Times

The quality changes of the 1 mm (a), 1.5 mm (b), and 2 mm (c) PNIPAm/PPy hydrogels before and after hygroscopy are shown in Figure 10 and Table 4, and the appearance quality of PNIPAm/PPy is shown in Figure 10. As can be seen from Table 4, the moisture absorption amount barely decreased. Although the mass of the 2 mm PNIPAm/PPy hydrogel decreased by 0.0001 g on its 20th use, we believe that the mass has not changed due to the error of the balance being  $\pm 0.0002$  g. Figure 11 shows the material after its 20th use. The density of the material does not change. Although the mass of the 2 mm PNIPAm/PPy hydrogel decreased by 0.0001 g on its 20th use, this is a statistically insignificant difference. Thus, PNIPAm/PPy has good regeneration performance and can be reused multiple times.



**Figure 10.** Changes in weight of materials before and after moisture absorption with regeneration times. (a) The weight of PNIPAm/PPy before and after multiple hygroscopic processes (1 mm). (b) The weight of PNIPAm/PPy before and after multiple hygroscopic processes (1.5 mm). (c) The weight of PNIPAm/PPy before and after multiple hygroscopic processes (2 mm).

**Table 4.** Changes in weight of materials before and after moisture absorption with regeneration times.

Size	Number of experiments	Weight (g)					
		1 mm		1.5 mm		2 mm	
		Before	After	Before	After	Before	After
	0	0.1198	0.6518	0.1796	0.9897	0.2395	1.3022
	5	0.1198	0.6518	0.1796	0.9897	0.2395	1.3022
	10	0.1198	0.6518	0.1796	0.9897	0.2395	1.3022
	15	0.1198	0.6518	0.1796	0.9897	0.2395	1.3022
	20	0.1198	0.6518	0.1796	0.9897	0.2394	1.3021



**Figure 11.** Photos of PNIPAm/PPy before and after material desorption (20 times; thickness of 2 mm).

The experimental results show that the PNIPAm/PPy hydrogel has good regeneration performance and can be used repeatedly, which greatly reduces the cost of hygroscopic materials.

#### 4.4. Energy Savings Analysis

Silica gel and zeolite are the most commonly applied materials in solid adsorption dehumidification systems. Therefore, silica gel was selected as a reference for performance comparison. Table 5 shows the comparison of the performance parameters of the 2 mm PNIPAm/PPy hydrogel and traditional silica gel under the same operating conditions. It can be seen that when the moisture absorption efficiency reaches 80% (as shown in Section 4.2.1), the unit equilibrium moisture absorption of this material at 26 °C and an RH = 60% is 3.72 g/g, while this value is 0.281 g/g for silica gel [25]. The unit equilibrium moisture absorption increased 12.2-fold. The lowest desorption temperature of PNIPAm/PPy was 40 °C, while this value was 120 °C for silica gel. The desorption temperature was reduced by 80 °C. At 60 °C, the effective desorption time of PNIPAm/PPy was 120 min, and the same value for silica gel was 480 min. Therefore, the application of these materials in solid dehumidification systems can not only improve moisture absorption but also greatly reduce the amount of energy consumed by a building's dehumidification.

**Table 5.** Comparison of performance parameters between PNIPAm/PPy and traditional silica gel.

	Hygroscopicity (g/g)	Minimum Desorption Temperature (°C)	Effective Desorption Time (min, at a Temperature of 60 °C)
PNIPAm/PPy	3.720	40	120
Silica gel	0.281	120	480

As shown above, PNIPAm/PPy has good moisture absorption and regeneration performance. Therefore, it has good applicational prospects and can be vigorously promoted and applied to solid dehumidification systems. Shown in Figure 12, we designed an alternate solid dynamic adsorption dehumidification system with a sterilization function using the PNIPAm/PPy hydrogel, including a fresh air dehumidification subsystem, a sterilization and disinfection subsystem, and a returning air desorption subsystem [26].

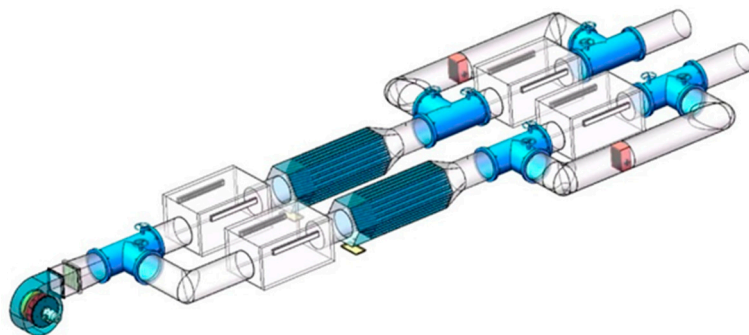


**Figure 12.** Schematic diagram of solid dehumidification system using PNIPAm/PPy.

The system involves an initial fresh air dehumidification process, a second fresh air dehumidification process, an initial mixed dehumidification process, and a second mixed dehumidification process. The first mixed dehumidification process consists of the second fresh air dehumidification process and the first return air desorption process, which are carried out simultaneously. The second mixed dehumidification process includes the first fresh air dehumidification process and the first desorption process, which are carried out simultaneously. The first mixed dehumidification process, the second fresh air dehumidification process, the second mixed dehumidification process, and the first fresh air dehumidification process operate in sequence and form a cycle.

## 5. Conclusions

In this paper, a PNIPAm/PPy hydrogel hygroscopic material was prepared; then, by testing and analyzing the properties of the PNIPAm/PPy hydrogel hygroscopic material, the following conclusions were drawn:

- (1) The pore structure of PNIPAm/PPy is complex, and there are abundant pores with uneven pore sizes. The minimum pore size is about 4  $\mu\text{m}$ , the maximum pore size is about 25  $\mu\text{m}$ , and the pore sizes are mostly distributed between 8 and 20  $\mu\text{m}$ . The hydrogel's abundant and dense pores grant it good hygroscopic and water-releasing properties. The PPy inside the hydrogel plays the role of a hygroscopic and photothermal agent.
- (2) The hygroscopic efficiency of PNIPAm/PPy reached 80% in air, attaining relative humidity values of 90%, 60%, and 50% in about 75, 100, and 120 min, corresponding to unit equilibrium hygroscopic capacities of 3.85 g/g, 3.72 g/g, and 3.71 g/g, respectively. In the initial stage, the moisture absorption increases with the increase in time; subsequently, the rate of increase in moisture absorption decreases. The higher the relative humidity, the faster the moisture absorption rate. When the temperature is below 40 °C, the hygroscopic performance of PNIPAm/PPy is almost temperature-independent. In addition, the moisture absorption efficiencies of PNIPAm/PPy with different thicknesses were similar.
- (3) The lowest desorption temperature of PNIPAm/PPy is 40 °C, and this lower desorption temperature indicates that low-grade energy can be used for desorption. The higher the temperature, the faster the desorption rate and the higher the desorption amount of PNIPAm/PPy. The faster desorption rate observed indicated that the use of PNIPAm/PPy greatly reduced the amount of energy consumed in the regeneration process of the solid dehumidification system.
- (4) Compared with traditional silica gel, it can be seen that when the hygroscopic efficiency reaches 80%, the unit equilibrium hygroscopic capacity of PNIPAm/PPy is increased 12.2-fold at 26 °C and a RH = 60%. The desorption temperature of the material is reduced by 80 °C. At the temperature of 60 °C, the effective desorption time was shortened by 360 min.

**Author Contributions:** Conceptualization, J.L. and Y.W.; methodology, Z.Z. (Zilong Zhong) and D.C.; validation, Z.Z. (Zhou Zhou); investigation, W.W. and S.M.; writing—original draft preparation, J.L. and Z.Z. (Zilong Zhong); writing—review and editing, Y.W.; supervision, Y.W.; funding acquisition, Y.W. and J.L. All authors have read and agreed to the published version of the manuscript.

**Funding:** This work is supported by the National Natural Science Foundation of China (Grant No. 51806096) and National College Student Innovation and Entrepreneurship Training Program (Grant No. 202210291036Z).

**Data Availability Statement:** Not applicable.

**Conflicts of Interest:** The authors declare no conflict of interest.

## References

1. Vakiloroyaya, V.; Samali, B.; Fakhar, A.; Pishghadam, K. A review of different strategies for HVAC energy saving. *Energy Convers. Manag.* **2014**, *77*, 738–754. [[CrossRef](#)]
2. Cao, X.; Dai, X.; Liu, J. Building energy-consumption status worldwide and the state-of-the-art technologies for zero-energy buildings during the past decade. *Energy Build.* **2016**, *128*, 198–213. [[CrossRef](#)]
3. Zhang, L.; Jiang, Y.; Zhang, Y. Membrane-based humidity pump: Performance and limitations. *J. Membr. Sci.* **2000**, *171*, 207–216. [[CrossRef](#)]
4. Liu, J.L. Experimental Study on the Performance of Solid Adsorption Indoor Air Dehumidification Materials. Master's Thesis, Beijing University of Civil Engineering and Architecture, Beijing, China, 2020.
5. Rao, Z.; Wang, S.; Zhang, Z. Energy saving latent heat storage and environmental friendly humidity-controlled materials for indoor climate. *Renew. Sustain. Energy Rev.* **2012**, *16*, 3136–3145. [[CrossRef](#)]
6. La, D.; Dai, Y.; Li, Y.; Wang, R.; Ge, T. Technical development of rotary desiccant dehumidification and air conditioning: A review. *Renew. Sustain. Energy Rev.* **2010**, *14*, 130–147. [[CrossRef](#)]

7. WHO. *Ambient Air Pollution: A Global Assessment of Exposure and Burden of Disease*; World Health Organization: Geneva, Switzerland, 2016.
8. Jin, S.X.; Yu, Q.F.; Li, M.; Sun, S.N.; Zhao, H.; Huang, Y.W.; Fan, J. Quantitative evaluation of carbon materials for humidity buffering in a novel dehumidification shutter system powered by solar energy. *Build. Environ.* **2021**, *194*, 107714. [[CrossRef](#)]
9. Jeong, J.; Yamaguchi, S.; Saito, K.; Kawai, S. Performance analysis of desiccant dehumidification systems driven by low-grade heat source. *Int. J. Refrig.* **2011**, *34*, 928–945. [[CrossRef](#)]
10. Yaningsih, T. Analysis of heat and mass transfer characteristics of desiccant dehumidifier system with honeycomb configuration. *Appl. Therm. Eng. Des. Process. Equip. Econ.* **2018**, *144*, 658–669. [[CrossRef](#)]
11. Kumar, S.R.; Pillai, P.K.; Warriar KG, K. Synthesis of high surface area silica by solvent exchange in alkoxy derived silica gels. *Polyhedron* **1998**, *17*, 1699–1703. [[CrossRef](#)]
12. Chung, T.W.; Yeh, T.S.; Yang, C.K. Influence of manufacturing variables on surface properties and dynamic adsorption properties of silica gels. *J. Non-Cryst. Solids* **2001**, *279*, 145–153. [[CrossRef](#)]
13. Kuma, T. Active Gas Absorbing Element and Method of Manufacturing. US Patent US4886769A, 12 December 1989.
14. Djaeni, M.; van Boxtel, A.J.B.; Wang, J. Development of a new High Energy efficiency zeolite food adsorption Dryer. *Dry. Technol. Equip.* **2013**, *11*, 7–13.
15. Tokarev, M.; Gordeeva, L.; Romannikov, V.; Glaznev, I.; Aristov, Y. New composite sorbent CaCl<sub>2</sub> in mesopores for sorption cooling/heating. *Int. J. Therm. Sci.* **2002**, *41*, 470–474. [[CrossRef](#)]
16. Griesinger, A.; Spindler, K.; Hahne, E. Measurements and theoretical modelling of the effective thermal conductivity of zeolites. *Int. J. Heat Mass Transf.* **1999**, *42*, 4363–4374. [[CrossRef](#)]
17. Bareschino, P.; Diglio, G.; Pepe, F.; Angrisani, G.; Roselli, C.; Sasso, M. Numerical Study of a MIL101 Metal Organic Framework Based Desiccant Cooling System for Air Conditioning Applications. *Appl. Therm. Eng.* **2017**, *124*, 641–651. [[CrossRef](#)]
18. Canivet, J.; Fateeva, A.; Guo, Y.; Coasne, B.; Farrusseng, D. Water adsorption in MOFs: Fundamentals and applications. *Chem. Soc. Rev.* **2014**, *43*, 5594–5617. [[CrossRef](#)]
19. Yoshida, R.; Uchida, K.; Kaneko, Y.; Sakai, K.; Kikuchi, A.; Sakurai, Y.; Okano, T. Comb-type grafted hydrogels with rapid de-swelling response to temperature changes. *Nature* **1995**, *374*, 240–242. [[CrossRef](#)]
20. Wu, X.S.; Hoffman, A.S.; Yager, P. Synthesis and characterization of thermally reversible macroporous poly(N-isopropylacrylamide) hydrogels. *J. Polym. Sci. Part A Polym. Chem.* **1992**, *30*, 2121–2129. [[CrossRef](#)]
21. Zhao, F.; Zhou, X.; Liu, Y.; Shi, Y.; Dai, Y.; Yu, G. Super Moisture-Absorbent Gels for All-Weather Atmospheric Water Harvesting. *Adv. Mater.* **2019**, *31*, 1806446. [[CrossRef](#)]
22. Winnik, F.M. Fluorescence studies of aqueous solutions of poly(N-isopropylacrylamide) below and above their LCST. *Macromolecules* **1990**, *23*, 233–242. [[CrossRef](#)]
23. Ramaprasad, A.; Latha, D.; Rao, V. Synthesis and characterization of polypyrrole grafted chitin. *J. Phys. Chem. Solids* **2017**, *104*, 169–174. [[CrossRef](#)]
24. Yang, H.; Song, Y.X.; Xu, S.Q.; Yang, S.; Xiang, R.; Zheng, Z. Preparation and performance study of calcium chloride modified silicone hygroscopic material. *Packag. Eng.* **2022**, *43*, 216–225.
25. Liu, L.L.; Wang, G.; Wang, Z.; Hu, N. Experimental study on hygroscopic performance and regeneration effect of several common solid adsorbents. *J. Anhui Jianzhu Univ.* **2019**, *27*, 6. (In Chinese)
26. Zhong, Z.L.; Wang, Y.; Liu, J.L.; Zhou, D.; Mai, S. A Honeycomb Type Indoor Air Alternating Dehumidification System and Method with Sterilization Function. China CN115717746A, 28 February 2023.

**Disclaimer/Publisher’s Note:** The statements, opinions and data contained in all publications are solely those of the individual author(s) and contributor(s) and not of MDPI and/or the editor(s). MDPI and/or the editor(s) disclaim responsibility for any injury to people or property resulting from any ideas, methods, instructions or products referred to in the content.